Anomalous reduction in thrust/reaction of water jets issuing from microapertures

Tomiichi Hasegawa[a)]
Faculty of Engineering, Department of Mechanical and Production Engineering, Niigata University, Ikarashi-2, 950-2181 Niigata-shi, Japan

Hiroshi Watanabe
Niigata TLO, Ikarashi-2, Niigata University, 950-2181 Niigata-shi, Japan

Takashi Sato, Tohru Watanabe, and Masanao Takahashi
Graduate School of Science and Technology, Niigata University, Ikarashi-2, 950-2181 Niigata-shi, Japan

Takatsune Narumi
Faculty of Engineering, Department of Mechanical and Production Engineering, Niigata University, Ikarashi-2, 950-2181 Niigata-shi, Japan

Carlos Tiu
Department of Chemical Engineering, Monash University, Clayton, Vic. 3800, Australia

(Received 23 October 2006; accepted 19 March 2007; published online 4 May 2007)

Thrusts and reactions of water jets issuing through small orifices and thin slots were measured and compared with the predictions from numerical solutions of the Navier-Stokes equations. Reasonable agreements were obtained between the experimental and numerical results for orifices and slots with openings of the order of 1 mm size, but not with those of 10 μm or less. The experimental results were found to be well below the predictions for apertures of the order of 10 μm. The difference between the numerically calculated and the measured thrusts/reactions for the small apertures was found to be proportional to the square of the mean velocity. Several possible causes for the observed reduction in jet thrust/reaction in small apertures were examined, but none of them could adequately explain the flow anomaly. © *2007 American Institute of Physics*. [DOI: 10.1063/1.2723642]

I. INTRODUCTION

In recent years, much attention has been focused on the flow through microchannels in experiments of chemical and biochemical processes. A microchannel is usually defined as a channel of scale less than 1 mm. There have been numerous experimental investigations for this type of flow in the literature. Oliver and McSporran[1–3] insisted that the jet thrust method could be used to detect small fluid elasticity due to the high strain rates generated in such a flow. Measurements of the jet thrust of water and organic liquids issuing from a capillary into an air environment were found to be smaller than those predicted from Poiseuille flow. They concluded that even water and low molecular weight organic liquids could exhibit elastic properties at certain strain rates. However, their correction for the surface tension has been open to debate. Hasegawa[4] examined the jet reaction of a water jet issuing from a capillary tube into a vessel containing water, and found similar results to those obtained by Oliver and McSporran. The results were used to estimate the elastic stress of water in shear flow. These pioneered works have not been accepted widely due to the diversity of experimental data and the controversy of results. More recently, Hasegawa *et al.*[5] measured pressure drops for water flowing through small orifices ranging from 1.0 mm to 10 μm. They found that the excess pressure drop in orifice flow increased markedly when the orifice diameter was less than 50 μm. The increase in the excess pressure drop could not be explained from the numerical solution of the Navier-Stokes equation. They have raised the question on the applicability of the Navier-Stokes equations in small channel flows. Hsiai *et al.*[6] measured the total pressure drops of water flow through micromachined particle filters. Their experimental results compared reasonably well with numerical simulations. Mala and Li[7] measured flow rates and pressure drops for water flowing through microtubes and found that the experimental results departed significantly from theoretical predictions. Janssens-Maenhout and Schulenberg[8] used the concept of diffusive electrical double layers to explain the increase in pressure drop, but the predicted increase was far removed from the experimental value. On the other hand, Herwig and Hausner[9] insisted that the unusual results could be explained by conventional fluid mechanics, although this was critically challenged by Gad-el-Hak.[10] Gad-el-Hak[11] also reviewed a number of contradictory experimental results of liquid flow in microdevices. It appears that the flow behavior of liquids in microchannels remains unclear. Perhaps using a more rigorous non-Newtonian rheological model in the equation of motion may provide an answer to the observed anomalous behavior.

In the present study, jet reaction and jet thrust experiments are carried out using various Newtonian liquids flowing through small orifices and thin slots. The results are com-

[a)]Author to whom correspondence should be addressed. Electronic mail: hasegawa@eng.niigata-u.ac.jp

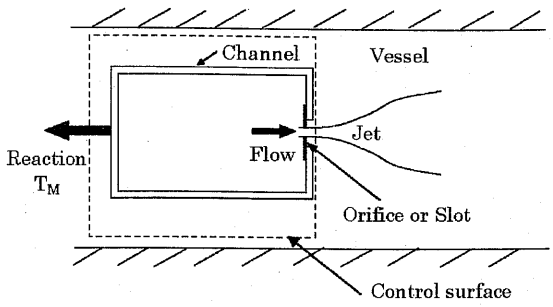

FIG. 1. Experimental arrangement for measuring jet reactions.

pared with the numerical solutions of the Navier-Stokes equation.

II. EXPERIMENT

A. Jet reaction method

The jet reaction apparatus utilized the torsion of a tube to measure the reaction of the jet (T_M) issuing from an orifice or a slot, which was attached at the end of the flow channel. Figure 1 is a conceptual representation of the flow channel immersed in the liquid vessel as used in the experiment. The measured force is termed the jet reaction or simply the reaction. The schematic diagram of the apparatus is shown in Fig. 2(a). Test fluid was supplied with a syringe pump, and flowed through a torsion tube, a turning center, and a brass tube, then ejected as a liquid jet from the orifice or slot attached to the end of the flow channel into the liquid in a vessel. Smaller jet reactions on the torsion tube were detected with a laser displacement sensor installed against the reflection arm, as shown in Fig. 2(a), whereas larger jet reactions were measured with a load cell connected to the end of the brass tube. The position of the load cell was adjusted to ensure that there was no torsion experienced in the torsion tube (the so-called zero method), as shown in Fig. 2(b). It was confirmed that both measuring techniques gave the same degree of accuracy for intermediate values of jet reaction. The outputs of the load cell and the laser displacement sensor were connected to a PC with an A/D converter. The whole measuring system was enclosed in a box to protect against wind disturbance.

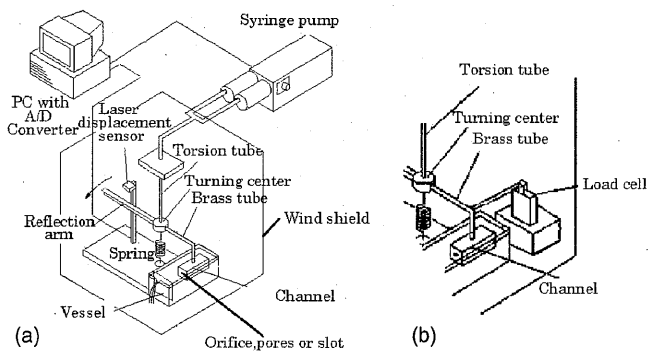

FIG. 2. Schematic diagram of the experimental apparatus. (a) Measurement by torsion. (b) Measurement by load cell.

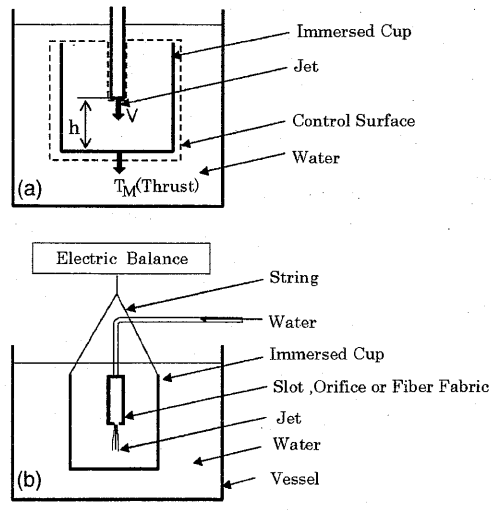

FIG. 3. Explanatory figures of the experimental apparatus for the jet thrust method. (a) Measuring principle. (b) Schema of the setup in experiments.

B. Jet thrust method

Another experimental method was adopted for measuring the jet thrust. The apparatus is schematically shown in Figs. 3(a) and 3(b). A jet of water was issued from the apertures into a cup, which was immersed in a vessel filled with water. Since the opening area of the cup is much larger than the cross-sectional area of the jet, the momentum flux flowing out of the cup can be neglected relative to the momentum of the jet. The force measured by this method (T_M) is called the jet thrust or simply the thrust. The cup was suspended by strings connected to an electric balance for measuring the force T_M. The cup was made of a material only marginally heavier than water, in order to lessen the extra weight working on the balance.

The validity of this apparatus was experimentally confirmed by comparison with the theoretical predictions. As shown in Fig. 4, the dimensionless thrust $T_M/\rho QV$ (where ρ is the density, Q is the flow rate, V is the mean velocity) is independent of the distance h between the aperture and the bottom of the cup and agrees with the theoretical value of

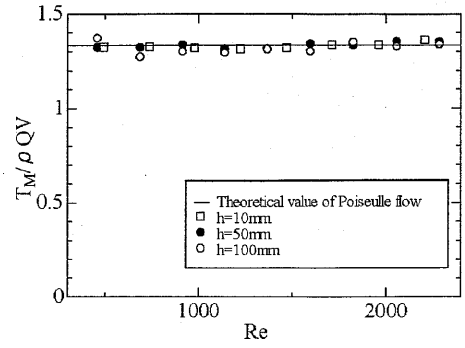

FIG. 4. Dimensionless measured thrust ($T_M/\rho QV$) vs Reynolds number ($\mathrm{Re}=Vd/\nu$) for tube flows. A solid line shows the value (1.33) of Poiseuille flow. h represents the distance between the tube tip and the cup bottom. The tube diameter is 1.2 mm.

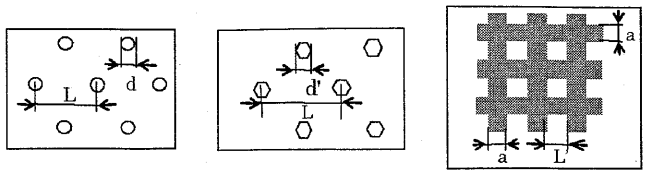

(a) Pores ; d=4.9μm L_1=35μm L_1/d=7.1

(b) Hexagonal Pores ; d'=35μm , L_2=130μm L_2/d'=3.7

(c) Fiber fabric ; a=46μm , L'=49μm

FIG. 5. Details of the pores used.

1.33 as predicted from the Poiseuille flow, almost independent of Reynolds number Re(=Vd/ν) (where d is the tube diameter and ν is the kinematic viscosity).

C. Apertures and liquids

The small apertures used in this study consisted of stainless steel orifice plates of diameter 1.2 to 0.50 mm and thickness 50 μm; 55 600 pores of diameter 4.9 μm regularly spaced on a thin, circular nickel disk with a diameter of 8 mm and a thickness of 11 μm [Fig. 5(a)]; regular arrays of 35.0 μm hexagonal pores [Fig. 5(b)] on a 40 μm thick nickel sheet; and a screen mesh of polyester fabric fiber with a width of 46 μm having square openings of 49×49 μm [Fig. 5(c)]. In addition, a set of stainless steel slots, consisting of slots of 24, 131, 292 μm wide and 200 μm thick slots, and 16 and 971 μm wide and 300 μm thick slots, was also used in the experiment. All slots were 20 mm in length. The larger orifices of diameter 1.2 to 0.5 mm, and all of the slots used were straight drilled or cut holes of normal wedge angle. The 4.9 μm pores and 35 μm hexagonal pores had round corners. In addition, the fiber fabric consisted of the squares was partitioned by four threads of diameter 46 μm and had round inlets. Dimensions of pores were measured by using digital microscope.

The test liquids used were water, silicon oil, liquid paraffin, and an aqueous KCl solution. Special attention was paid to maintain the purity of the water flowing through small pores. All test water was distilled, deionized, and filtered before the jet reaction/thrust experiments. The flow rate was accurately measured by adjusting the dial of the syringe pump, where calibration had been made beforehand between the dial and the flow rate obtained by weighing the liquid discharged over a given time period. The pump output was repeatedly checked for leakage, because it was generally operated at high pressure in order to force the liquid through the small orifices and slots.

In the preliminary test, colored water was used for visualization of the water jet issuing from the slot exit into a water bath. Proper setting of slots was confirmed when the observed colored jet stream was straight. Fluctuations were often observed in the outputs of jet reaction. Overall, a 10% error was estimated in the measurements of reaction forces for smaller apertures. This magnitude of error, however, was found to have no significant effect on the final result.

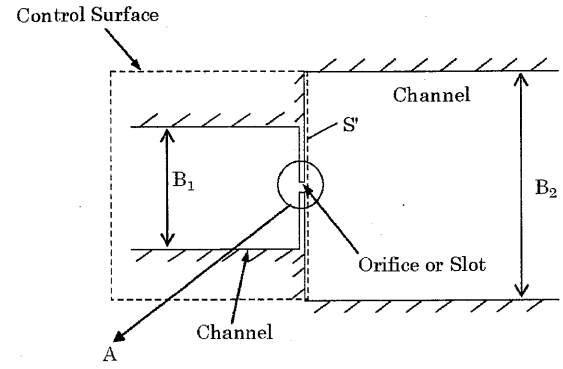

FIG. 6. The configuration used for numerical analysis. B_1 is the upstream width and B_2 is the downstream width of the channel. S' is a part of the control surface that coincides with the end surface of the downstream channel. In the present apparatus, the upstream channel is 25 mm wide, and the vessel is 220 mm wide.

III. NUMERICAL ANALYSIS

The finite element method was used for numerical analysis of Newtonian fluids, in which velocities and pressures were expressed with interpolation functions in finite elements. The Galarkin method was adopted to obtain the discretized ordinary differential equations, which were solved using the Newton-Raphson method. A mixed method was used to solve the pressure field. Both velocity and pressure were assumed to be continuous at the boundary of the elements. The analysis was carried out using a commercial software package FIDAP of Fluid Dynamics International, Inc.

Figure 6 shows the model flow channel used for the numerical analysis. The upstream and downstream widths are represented by symbols B1 and B2, respectively. The following boundary conditions are assumed: (a) Poiseuille flow existed at the inlet boundary, (b) the pressure and the velocity in the r direction are zero at the outlet boundary, (c) the r component of the velocity is zero on the center line, and (d) all velocities are zero at the wall (no slip). Figure 7 shows the three different configurations used in numerical calculations. Figure 7(a) represents Case 1, in which the fluid flows through an orifice of diameter d or a slot of width b on a

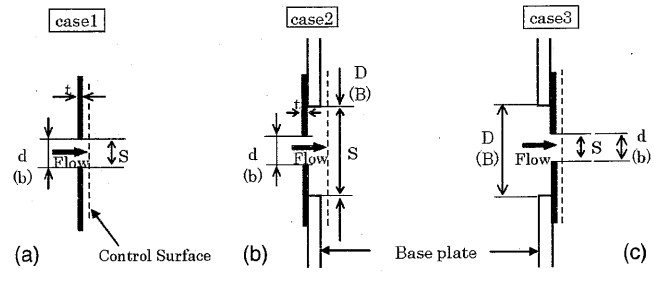

FIG. 7. Details of orifice or slot setting to the base plate (part A in Fig. 6). (a) Case 1, (b) Case 2, and (c) Case 3. d and b are the orifice diameter and slot width, respectively, S is the surface area of the hole opened at the downstream side, D and B are the larger hole diameter and slot width, respectively at the downstream side (D=10 mm for the 0.5 to 1.2 mm orifices or 1 mm for the pores and fiber fabric, and B=4 mm for the slots). The thickness t is 50 μm for the larger orifices, 0.2 or 0.3 mm for slots, 11 μm for the membrane of circular pores, and 40 μm for the membrane of hexagonal pores.

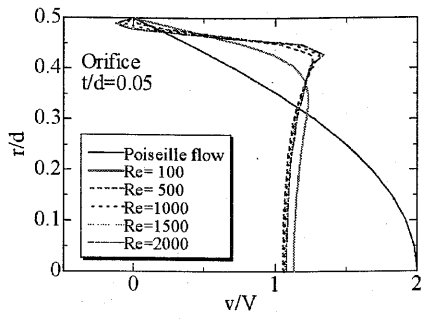

FIG. 8. Velocity profiles calculated at the exit of an orifice.

plate of thickness t; Fig. 7(b) shows that an orifice or a slot is attached over a larger hole of diameter D or a wider slot of width B drilled into the base plate, respectively (Case 2); and Case 3 is the mirror image of Case 2, in which the fluid is flowing in the opposite direction [Fig. 7(c)]. Although all three cases were considered in the numerical analysis, flow experiments were carried out only in orifices and/or slots arranged in either Case 2 or 3. The dotted lines on the figures represent a part of the control surface used for the calculation of jet reaction.

The calculated reaction or thrust T_N for Newtonian fluids is obtained by applying the momentum balance on the control surface as

$$T_N = \rho \int_S v^2 dA + \int_{S'} p dA - 2\mu \int_{S'} \frac{\partial v}{\partial x} dA, \tag{1}$$

where v is the local velocity in the flow direction (x component) normal to the exit plane; S is the opening area of the orifice or slot (Cases 1 and 3) or the area of the larger hole or slot in Case 2; S' is the entire surface on the right-hand side (RHS) of the control surface including S, and p is the pressure at any position on S'. The last term on the RHS of Eq. (1) represents the normal force due to the fluid normal stress, which is equal to $2\mu\partial v/\partial x$ for Newtonian fluids.

IV. RESULTS AND DISCUSSION

A. Numerical results

Figure 8 presents the calculated velocity profile (v/V) against the radial position (r/d) at the exit plane of an orifice having a thickness ratio t/d=0.05, at different Reynolds numbers. It is seen that the dimensionless maximum velocity at the center line decreases as Reynolds number increases, and a concave-type velocity profile in the central region is predicted at Reynolds numbers greater than 100. Furthermore, a reverse flow near the wall region is observed at high Reynolds number above 500. This kind of concave velocity profile has been reported in the literature.[12,13]

Figures 9(a) and 9(b) show the relative magnitudes of various momentum flux or force terms in Eq. (1) for orifice and slot flows, respectively. While the convective momentum flux term is nearly constant over the entire Re range for both orifice and slot flows, the pressure term is negative at low Re, and approaches zero when Re$>$50 in slot flow, but is positive when Re exceeds 100 in orifice flow. Finally, the

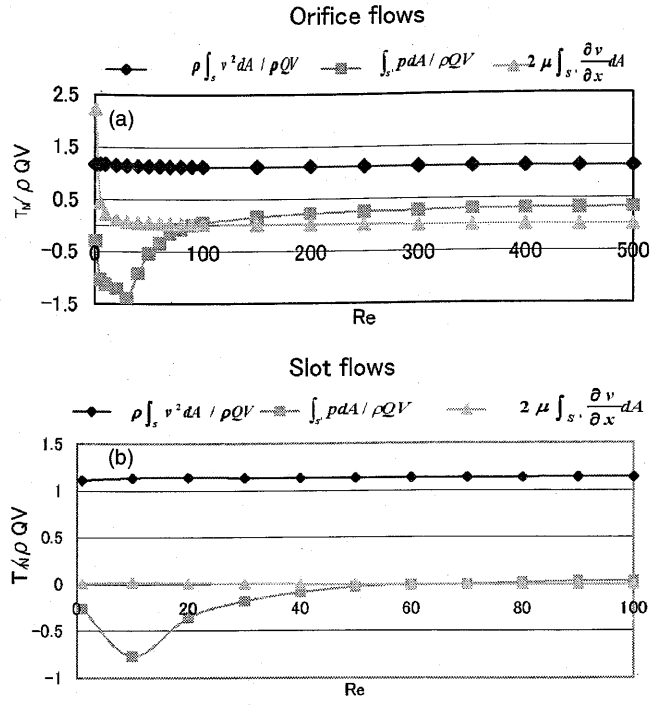

FIG. 9. Ratios of each term in the RHS of Eq. (1). (a) Orifice flows and (b) slot flows.

contribution of the viscous momentum flux is negligible compared to the other two terms. The predicted reaction/thrust T_N is compared with the measured T_M.

It is thought that the jet reaction may be affected by several geometric aspect ratios, such as B_1/d, B_2/d, and D/d, in Cases (1), (2), and (3). However, the numerical solution reveals that the geometric ratios B_1/d and B_2/d over the range $25 \leq B_1/d \leq 625$ and $220 \leq B_2/d \leq 5500$ have little effect on the reaction, but T_N is affected by the thickness ratio t/d, as seen in Figs. 10(a)-1 and 10(a)-2, and the calculated reaction decreases with increasing thickness ratio or decreasing pore size.

The mesh size used for the finite element calculation may also affect the predicted reaction. In order to capture the high elongation of fluid elements near the exit corner, it may be necessary to use a finer mesh size in the corner region. However, numerical solutions obtained using both coarse and fine mesh sizes indicate no discernible difference in the calculated reactions over a wide range of Reynolds number except at low Re. At Re$<$30, the prediction from the fine-mesh solution is about 10% higher than the coarse-mesh solution. Since most of the experiments were conducted in the high Re range, the coarse-mesh solution was deemed to be accurate enough for comparison purposes.

B. Experimental results

Experimental results of reaction/thrust are presented in the form of the dimensionless reaction/thrust force $T_M/\rho QV$ versus Reynolds number Re in Fig. 10. For comparison purposes, the numerically calculated jet reaction force T_N, is also included in the figure. As shown in Figs. 10(a)-1 and 10(a)-2, the measured reactions for various Newtonian liq-

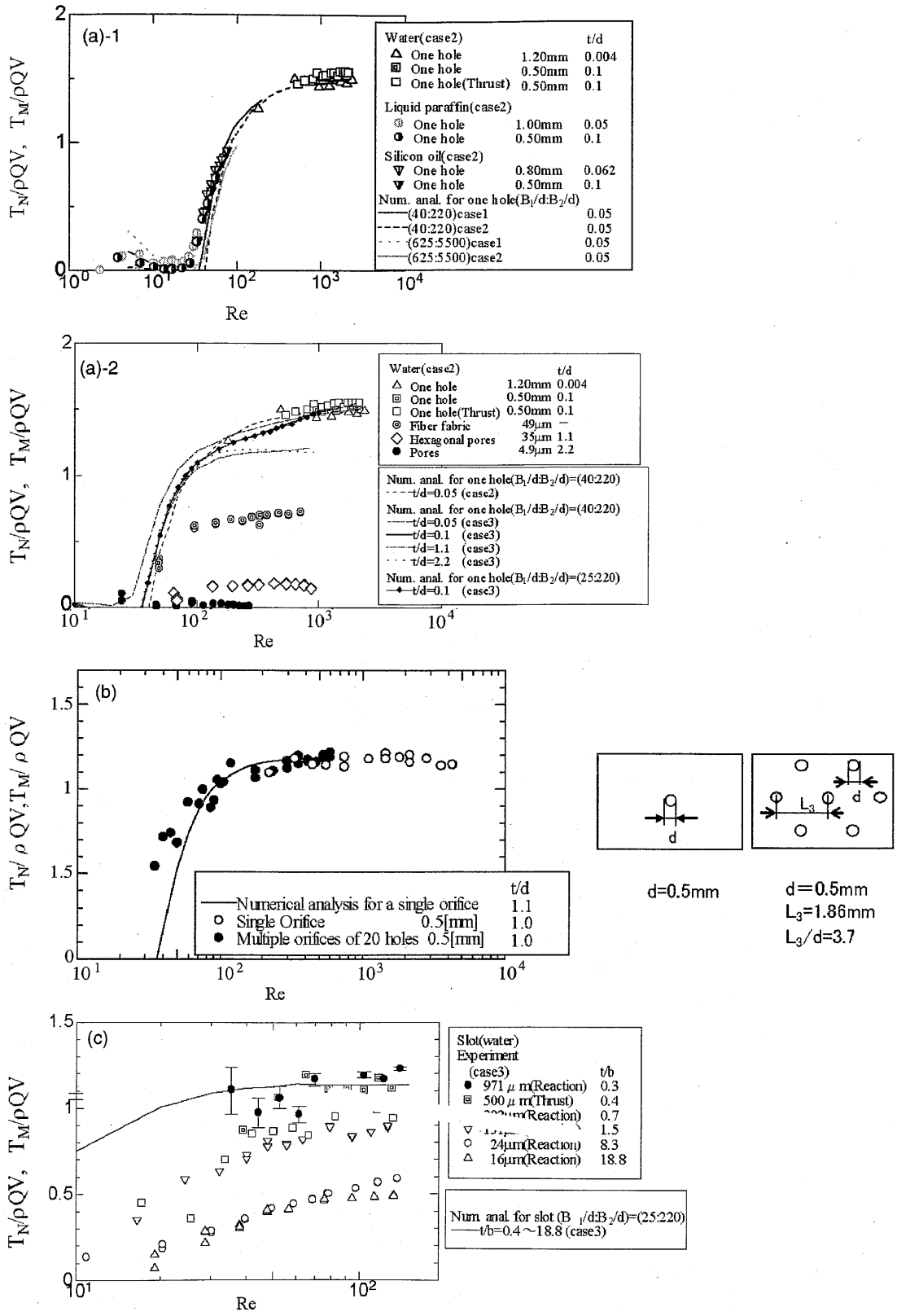

FIG. 10. Dimensionless reactions/thrusts obtained by experiments (keys) and numerical analysis (lines). (a) Reactions: Orifice flows: (1) Larger orifices, (2) Larger orifices, smaller pores, and fiber fabric for water. (b) Thrusts: Single and multiple orifices of the common diameter 0.5 mm. (c) Slot flows for water. The liquids used are water, liquid paraffin (ρ=860 kg/m^3, ν=81×10^{-6} m^2/s), silicon oil (ρ=955 kg/m^3, ν=30×10^{-6} m^2/s). The temperature ranges from 17 to 23 °C.

uids agree well with the numerical predictions for larger orifices (of diameters greater than 0.50 mm), but T_M are significantly lower than T_N for smaller aperture orifices (of diameter less than 50 μm). The measured dimensionless reactions are nearly independent of Reynolds number up to Re≈200 for the smaller pores, having a value of close to zero for the 4.9 μm pores, 0.2 and 0.6 for the 35 μm membrane and the 49 μm fabric, respectively. It was initially

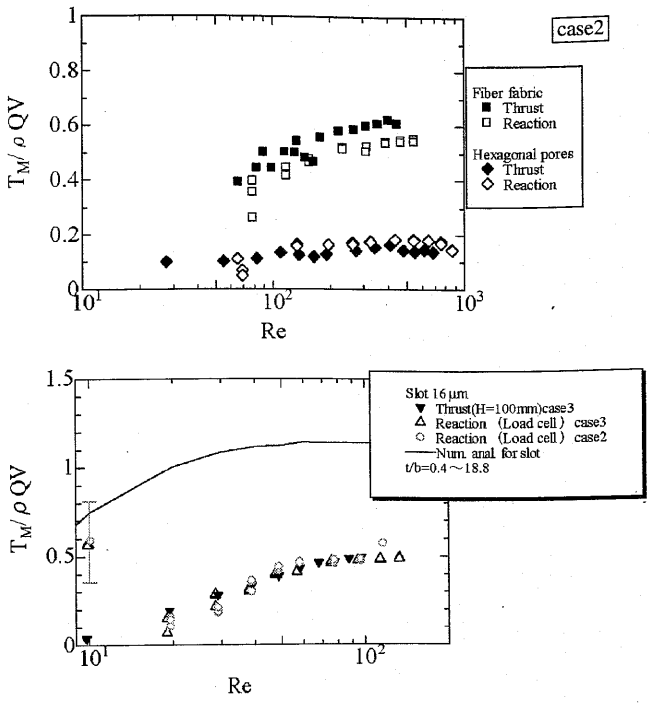

FIG. 11. Comparison between the reaction method and the thrust method. (a) Hexagonal pores and fiber fabric. (b) Slots.

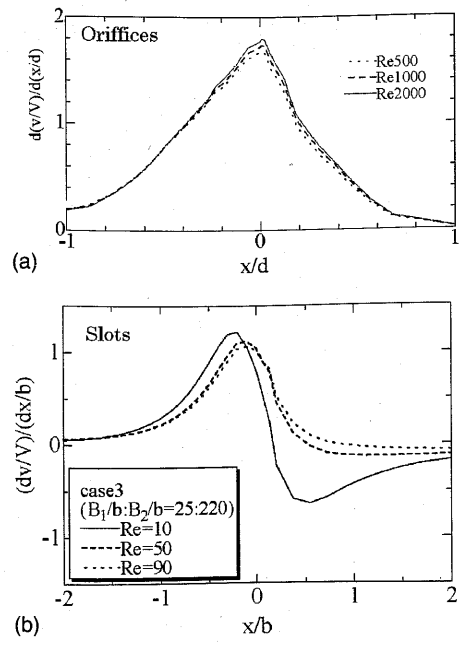

FIG. 12. Calculated dimensionless elongational rates on the center line. x is the distance measured from the entrance of the aperture. (a) Orifice flows. (b) Slot flows.

thought that the large discrepancy between the experimental and the predicted reactions for smaller pores could be due to the inaccuracy in data collection and the analytical techniques used in the experiments. The experimental uncertainties were evaluated by repeating the jet thrust experiments using a single orifice and multiple orifices of the same diameter (0.5 mm), as indicated by the hollow and solid circles, respectively, in Fig. 10(b). The multiple orifices consisted of 20 holes of 0.5 mm diameter and the array of the holes mimics the hexagonal pores (see Fig. 5). In both cases, the measured thrusts agree well with the numerical predictions. Therefore, any experimental errors due to the use of multiple holes for smaller orifices are negligible.

Figure 10(c) shows the dimensionless reaction for slot flows as a function of Reynolds number ($\mathrm{Re}=Vb/\nu$) obtained for Case 3. As in the case for orifice flow, reasonable agreements between the measured and predicted reactions are obtained for the larger slots (971 μm and 500 μm), but not for the smaller slots. The difference between T_M and T_N appears to increase with decreasing slot size.

Figures 11(a) and 11(b) show the experimental results obtained by both the reaction and the thrust methods for the hexagonal pores and the fiber fabric, and for the smaller slot, respectively. It is seen that the two methods yield almost identical results. For brevity, the term "thrust" refers to either "reaction" or "thrust" results hereafter. Figure 11(b) also reveals that the experimental values are significantly lower than the predicted values for the smaller slot. As seen from these figures, reproducibility of the data was fairly good.

In summary, the measured jet reactions or thrusts were found to agree reasonably well with the predicted values for apertures of the order of 1 mm size, but deviated considerably for smaller apertures of the order of 10 μm size.

C. Correlations of experimental results

Attempts were made if any correlation existed between the rate of reduction in thrust, defined as $\mathrm{RRT}=(T_N-T_M)/A$, and the elongational rate or the velocity. The elongational rate can be estimated along the center line of the channel from the predicted velocity profile, as shown in Figs. 12(a) and 12(b) for the orifice ($t/d=0.05$) and the slot ($t/b=0.3$), respectively. The maximum elongational rates for orifices and slots are found to be

$$\dot{e}_o = 1.75\frac{V}{d} \tag{2a}$$

and

$$\dot{e}_s = 1.0\frac{V}{b}. \tag{2b}$$

The axial elongational rate at the centerline varies rapidly from its maximum at the entrance to zero at the exit plane of the orifice or slot. Since it was not possible to determine the variation of elongational rate in such complicated flow fields (see also Fig. 8), the maximum elongational rates calculated from Eqs. (2a) and (2b) were used for the correlation of experimental results. Figure 13 shows a plot of RRT against $\dot{e}_o$ or $\dot{e}_s$ for the orifice and slot flows. Separate straight lines were obtained for different sizes of pore (orifice) and slot, suggesting that such a correlation does not exist.

Figure 14 shows a plot of RRT against the mean velocity V through the aperture for all experimental results obtained with water in orifice and slot flows. Except for those data obtained in the larger slots (≥ 131 μm), a unique correlation appears to exist between RRT and V. The slope of the straight line is approximated to be 2, suggesting that RRT is proportional to V^2.

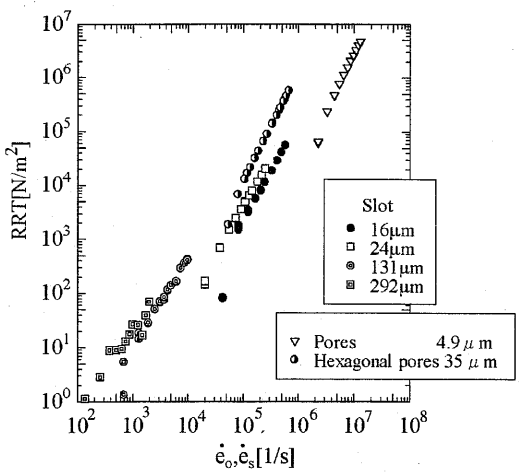

FIG. 13. Rate of reduction in thrust [RRT=$(T_N-T_M)/A$] vs the maximum elongational rates around the inlet ($\dot{e}_o$ for orifice flows or $\dot{e}_s$ for slot flows), where T_N is the predicted reaction or thrust for Newtonian fluids, T_M is the measured reaction or thrust, A is the cross-sectional area of the apertures, and $\dot{e}_o=1.75V/d$, and $\dot{e}_s=1.0V/b$.

D. Factors affecting the jet thrust measurements

It is clear from the experimental evidence presented above that there exists an anomalous flow behavior in microchannel flow with apertures of the order of 10 μm. Several factors that could cause this anomalous flow behavior are considered below.

1. Boundary slip

Recently, many researchers have focused their studies, both theoretically and experimentally, on the flow of liquids near the solid interface, in particular, the boundary slip exhibited by Newtonian liquids at the solid surface.[14] If boundary slip were to occur in the present flow systems, causing a reduction in pressure drop, the jet reaction measured for the

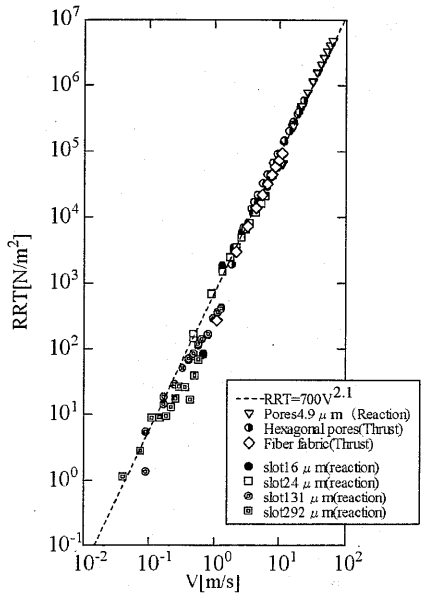

FIG. 14. RRT vs the velocity V for all the data in the present experiment. Dotted line is drawn so as to fit the experimental data.

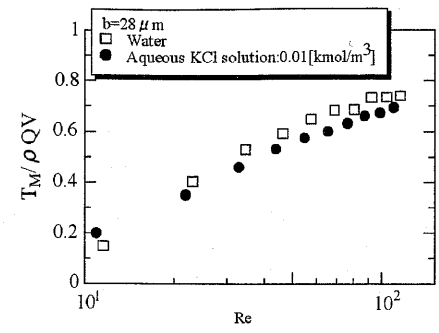

FIG. 15. Reactions of water and KCl 10^{-2} kmol/m^3 aqueous solution. Slot width is 28 μm.

case with wall slip would be smaller than the one without the wall slip. However, even allowing for slip flow, the maximum reduction in the reaction force would only be about $0.33\rho QV$. This estimate is based on the difference of momentum flux between a flat velocity profile for a complete slip flow and a parabolic profile for no-slip flow. In reality, the measured velocity profile for slip flow is far from being totally flat as assumed above.[15,16] Hence, boundary slip, even if it had occurred in the present flow system, would not be a main factor for the large decrease in the measured jet reaction/thrust.

2. Electroviscous effect

It has been reported[17] that when a liquid is forced through a microchannel by a hydrostatic pressure, the net charges carried by the flow outside the electrical double layer may induce a streaming potential. This streaming potential causes the flow in the opposite direction to the pressure-driven flow, resulting in a smaller net driving force. This is the so-called electroviscous effect. In order to assess the contribution of electroviscous effect, the jet reaction experiment was repeated using a 10^{-2} M KCl aqueous solution. Li[18] has obtained the lowest pressure gradient for the same concentration of KCl solution. The present results shown in Fig. 15 indicate that there is a small reduction in the measured reaction for the KCl solution as compared to pure water, but not to the extent of the discrepancy between the measured and predicted reactions in microchannel flow.

3. Fluid inertia

It has been shown in the preceding section that RRT is approximately proportional to the square of the mean velocity. This suggests that fluid inertia due to the change of velocity profile of the jet stream may play a role for the observed flow anomaly. It is assumed that the local velocity v varies from the mean velocity V by some function of radial position r,

$$v = V + f(r), \tag{3}$$

where $f(r)$ can be either positive or negative. The condition of continuity implies that

$$\int_0^R f(r)rdr = 0. \tag{4}$$

In orifice flows, the momentum flux M becomes

$$M = \rho QV + 2\pi\rho \int_0^R f^2 rdr. \tag{5}$$

Since the second term on the RHS of Eq. (5) is positive, the resulting momentum flux for the case of variable velocity profile is always larger than ρQV, or the momentum flux for the case of a flat velocity profile. In this case, the resulting reaction/thrust should be larger instead of smaller as indicated from the contribution of the first term on the RHS of Eq. (1). Therefore, the momentum flux caused by fluid inertia due to the variation of velocity profile cannot explain the present experimental result in microchannel flows.

V. CONCLUDING REMARKS

The reaction and thrust of water and some low molecular weight organic liquid jets flowing out of microsized orifices or slots were measured. The measured reactions/thrusts were found to deviate considerably and were much smaller than the numerical predictions from the Navier-Stokes equation for very small opening orifices and slots (<50 μm). Several factors including boundary slip, electroviscous and inertial effects that could influence the reduction in jet thrust in microaperture flows were considered in detail. However, they were found to be inappropriate to explain the flow anomaly.

ACKNOWLEDGMENT

The authors wish to thank Ryuichi Kayaba for technical assistance in carrying out the experiments.

[1]D. R. Oliver, "The expansion/contraction behavior of laminar liquid jets," Can. J. Chem. Eng., 100 (April 1966).
[2]D. R. Oliver and W. McSporran, "The expansion/contraction phenomenon in plane and circular jets," in *Deformation and Flow in High Polymer Systems*, Proceedings, Brit. Soc. Rheol. Conference on Deformation and Flow in High Polymer Systems, Loughborough, UK, 1966 (Macmillan, Basingstoke, 1968), p. 199.
[3]D. R. Oliver and W. McSporran, "Shear elasticity in organic liquids," Nature (London) **212**, 918 (1966).
[4]T. Hasegawa, "Measurement of the first normal stress differences of water and dilute polymer solutions," Bull. JSME **22**, 54 (1979).
[5]T. Hasegawa, M. Suganuma, H. Watanabe, "Anomaly of excess pressure drops of the flow through very small orifices," Phys. Fluids **9**, 1 (1997).
[6]T. K. Hsiai, S. K. Cho, J. M. Yang, X. Yang, Y. Tai, and C. Ho, "Pressure drops of water flow through micromachined particle filters," J. Fluids Eng. **124**, 1053 (2002).
[7]G. M. Mala and D. Li, "Flow characteristics of water in microtubes," Int. J. Heat Fluid Flow **20**, 142 (1999).
[8]G. G. A. Janssens-Maenhout and T. Schulenberg, "An alternative description of the interfacial energy of a liquid in contract with a solid," J. Colloid Interface Sci. **257**, 141 (2003).
[9]H. Herwig and O. Hausner, "Critical view on 'New results in microfluid mechanics': An example," Int. J. Heat Mass Transfer **46**, 935 (2003).
[10]M. Gad-el-Hak, "Comments on 'Critical view on new results in microfluid mechanics'," Int. J. Heat Mass Transfer **46**, 3941 (2003).
[11]M. Gad-el-Hak, "The fluid mechanics of microdevices: The Freeman Scholar Lecture," J. Fluids Eng. **121**, 5 (1999).
[12]J. S. Vrentas, J. L. Duda, and K. G. Bargeron, "Effect of diffusion of vorticity on flow development in circular conduits: Part 1. Numerical solutions," AIChE J. **12**, 837 (1966).
[13]E. B. Christiansen, S. J. Kelsey, and T. R. Carter, "Laminar tube flow through an abrupt contraction," AIChE J. **18**, 372 (1972).
[14]C. Neto, D. R. Evans, E. Bonaccurso, H.-J. Butt, and V. S. J. Craig, "Boundary slip in Newtonian liquids: a review of experimental studies," Rep. Prog. Phys. **68**, 2858 (2005).
[15]D. C. Tretheway and C. D. Meinhart, "Apparent fluid slip at hydrophobic microchannel walls," Phys. Fluids **14**, L9 (2002).
[16]D. C. Tretheway and C. D. Meinhart, "A generating mechanism for apparent fluid slip in hydrophobic microchannels," Phys. Fluids **16**, 1509 (2004).
[17]D. Li, "Electrokinetics in microfluidics," in *Interface Science and Technology*, Vol. 2 (Elsevier, New York, 2004), p. 86
[18]D. Li, "Electrokinetics in microfluidics," in *Interface Science and Technology*, Vol. 2 (Elsevier, New York, 2004), p. 68.